

Identification of heat-induced proteomes in meiotic pollen mother cells of tomato 'Maxifort' using single-cell-type tandem mass tag (TMT) proteomics

Hui Li¹, Yaoguo Qin¹, Xingbo Wu¹, Joshua O'Hair¹, Jesse Potts¹, Suping Zhou^{1*}, Yong Yang², Tara Fish², and Theodore W. Thannhauser^{2*}

¹ Department of Agricultural and Environmental Sciences, College of Agriculture, Tennessee State University, 3500 John A. Merritt Blvd, Nashville, TN 37209, USA

² Plant, Soil and Nutrition Research Unit, USDA-ARS, Tower Road, Ithaca, NY 14853, USA

* Corresponding authors, E-mail: zsuping@tnstate.edu; Ted.Thannhauser@ars.usda.gov

Abstract

Heat stress (HS) poses a significant challenge to tomato production due to disruption of the reproductive organs, especially the male gametophytes. This study reports HS-induced proteome changes in meiotic pollen mother cells during early stages of anther development. Tomato (*Solanum lycopersicum* L. × *S. habrochaites*) 'Maxifort' were grown in a heated polytunnel in Nashville, Tennessee, USA. Plants at flowering stage were subjected to heat treatment at 40 ± 2 °C for 4 hr (11:00–15:00 HR); and the non-heat-treated control was at 30 ± 2 °C (day/night) at the same period of time for 10 d. The size of the flower buds containing meiotic pollen mother cells was determined based on the histology of DAPI stained cross section of anthers. Flower buds were embedded in optimal cutting temperature solutions (OCT) and then cut into sections of 20 µm thickness. Sections containing meiotic pollen mother cells were collected using laser capture microdissection (LCM). A protein extraction procedure was optimized for the LCM collected pollen samples which yielded 25–30 µg protein from 150,000–200,000 pollen cells. The heat-induced proteomes of meiotic pollen mother cells were quantified using tandem mass tag (TMT) quantitative proteomics analysis. Among the 6,343 quantified proteins, 254 differentially expressed proteins (DEPs) showed significant differences in abundance level from heat treated to non-heat-treated control conditions. The heat-up-regulated-DEPs (96 proteins) include heat shock proteins, calreticulin and exocytosis (synaptobrevin) which are involved in protein folding/refolding/targeting/removal and secretion of aggregated and damaged proteins/peptides. The heat-down-regulated-DEPs (158 proteins) were involved in pathways of ubiquitin-mediated protein degradation, antioxidant mechanism, and metabolic processes of carbohydrates and lipids. Proteins affecting apoptotic programmed cell death and pollen mother cell meiotic activity were significantly changed under HS. The identified proteins and the affected biological processes could represent the major heat tolerance mechanisms during early developmental stages of male gametophyte when exposed to daily periods of above 40 °C HS condition.

Citation: Li H, Qin Y, Wu X, O'Hair J, Potts J, et al. 2022. Identification of heat-induced proteomes in meiotic pollen mother cells of tomato 'Maxifort' using single-cell-type tandem mass tag (TMT) proteomics. *Vegetable Research* 2:2 <https://doi.org/10.48130/VR-2022-0002>

INTRODUCTION

Tomato is one of the most important vegetable crops in the world with an annual value exceeding \$90 billion^[1]. In the US, fresh and processed tomatoes generate more than \$2 billion USD in annual farm cash receipts^[2]. Tomato production requires an optimum temperature range of 21–24 °C^[3]. In recent years, many tomato growing areas are experiencing hot summers when the field temperatures reach as high as 33–35 °C during the flowering and fruiting season. Under these high temperatures, photosynthesis and development of reproductive organs are both reduced, leading to low fruit-sets, low yield and poor fruit quality^[4–7]. Together with the demand for more water to maintain normal plant growth, rising temperatures have created a major challenge for summer tomatoes. This has created an urgent need for new genes and genetic materials to introduce heat stress (HS) tolerance into cultivated tomatoes.

Plants exposed to temperatures above certain thresholds for a period of time are experiencing HS which causes irreversible damage to plant physiological functions. Studies by Sato et al.

show that tomato plants exposed to 32/26 °C (d/n) for 10 d prior to anthesis produced low tomato fruit-set due to interruption of male reproductive development^[8,9]. Temperatures above 40 °C lasting for a few hours caused severe injuries to tomato plants leading to flower drop and interruption of fruit ripening^[10–12].

A number of studies have revealed that male gametophyte development is more susceptible to HS compared to female gametophyte cells^[13–15]. Tomato pollen grain formation is divided into the microsporogenesis and microgametogenesis phases. During the first phase, the reproductive diploid sporogenous cells first differentiate into pollen mother cells (PMCs, or pollen meiotocytes) which will undergo meiotic cell division to produce four haploid microspores (tetrads). In the second phase, microspores undergo two sequential mitosis cycles, which lead to the formation of trinucleate mature pollen containing one vegetative nucleus and two generative nuclei^[13,16]. The meiotic process of PMCs is the initial critical stage for plants to produce microspores. The meiotic PMCs were found to be extremely sensitive to temperatures above 40 °C^[8,17]. Exposure to such high heat, even for only a short-period of time, can

induce pollen meiosis abnormalities, tapetum development aberrations, and premature termination of microspore development^[14,18,19].

Tomato flowers take about 15 d from formation as inflorescence buds to fully opening (anthesis). The meiotic PMCs were observed in flower buds of 10–4 d before anthesis, which indicates that this stage occupies nearly 1/2 to 2/3 of the entire tomato flower developmental process (unpublished data, Li, Tennessee State University). It is well-understood that pollen cells beyond the microspore stage are highly sensitive to HS; loss of pollen viability and germination is the major factor causing low fruit-set and yield of tomatoes^[10,12]. However, in nature, hot days are periodic (they normally last for a few days to a week) and always alternate with cooler temperatures. Our hypothetical theory is that increasing the heat tolerance level of meiotic PMCs can enable the completion of the microsporogenesis process, and thus provide a constant supply of microspores during the hot days. As temperature drops, healthy pollen grain can be produced within 2–3 d to allow fruit-sets. Therefore, the HS tolerance of meiotic PMCs would provide an option for maintaining stable tomato production against periodic hot temperatures for summer tomatoes.

Tomato 'Maxifort' is used as a rootstock cultivar to improve tomato production under biotic (soilborne pathogens) and abiotic (salinity, heavy metals) stress conditions and maintain stable yield^[20,21]. We have observed that the 'Maxifort' plants were blooming vigorously in a polytunnel when the inside temperature reached above 40 °C during the hot summer. In this study, flower buds from this cultivar were collected to identify heat-induced proteomes in the meiotic PMCs. Even though the reproductive traits of this cultivar have little value in tomato production, the molecular mechanisms underlying the tolerance to high temperature can be very useful for improving heat tolerance during early flower development stages in cultivated tomatoes.

In flower anatomical structure, PMCs are embedded in anther locules which are comprised of several types of cells, each with distinct functions. Isolation of samples containing a homogeneous cell population has shown to be much more powerful for identifying genes/proteins specific to the biological function of the cells under investigation^[22,23]. This paper reports the isolation of meiotic PMCs using laser capture microdissection (LCM) followed by the identification of heat-induced proteomes using quantitative proteomics analysis. The primary objective is to provide the scientific community with a list of candidate genes (proteins) to be used to generate new and heat tolerant traits for tomatoes and other plants.

MATERIALS AND METHODS

Plant growth and heat stress treatments

Seeds of tomato 'Maxifort' were provided by Johnny's Selected Seeds (Winslow, ME). Tomato plants were grown in a heated polytunnel with no supplemental light on the Agricultural Research Station, Tennessee State University, Nashville, Tennessee. These tomato plants bloomed all year round; 16-month-old plants were used in this experiment. The temperature inside the polytunnel was controlled by rolling up and down the side curtains and recorded with mercury-based thermometers. The HS treatment was applied to keep the inside temperature at 40 ± 2 °C from 11:00 to 15:00 HR by

closing the side curtain. The temperature was above 30 °C at 9:00 and 18:00 HR (night temperature was not recorded). For the replace with non-HS-treated (N-HS) control condition, the polytunnel side-curtain was left open, the inside temperature was recorded at 30 ± 2 °C from 11:00 to 15:00 HR. The ambient average temperature during this treatment period was 31/20 °C (NOAA weather data). The treatments were applied for 10 d. Flower buds were taken at the end of each treatment period.

Identification of correlation between flower bud size and stage of pollen development

Flower clusters bearing the first opened flowers with many un-opened floral buds were taken from plants. To determine the correlation between flower bud size and the stage of pollen development, sepals and petals were removed, and the length of the stamens was measured from the base to the tip of the exposed flower stamen using an Insize vernier caliper. These flower buds were infiltrated in optimum cutting temperature (OCT) compound (Sakura, Torrance, CA) for 1 h, then embedded in OCT compound in 10 mm × 10 mm × 5 mm Tissue-Teck Cryomold (Sakura) and frozen into blocks under liquid nitrogen. Frozen flower buds were cross-sectioned into 20-µm thickness at –20 °C using a Leica CM1950 cryostat (Leica, Wetzlar, Germany), and then transferred to pre-coated adhesive slides (CFSA 1 X Slides) using CryoJane Tape-Transfer System. To determine pollen developmental stages, the cross-sections were stained in 4,6-diamidino-2-phenylindole (DAPI) (1 µg·mL⁻¹) in darkness for 15 min^[24]. The structure of anther locules and nuclei of pollen cells were observed and imaged under an upright microscope Axio Imager (M2; ZEISS, Oberkochen, Germany) using objective EC Plan-Neofluar 40x/0.75 M27 (FWD = 0.71 mm) and a BP335-383 excitation filter. The correlation between the size of the flower buds and pollen developmental stages was determined accordingly.

Collection of flower buds to isolate meiotic pollen mother cells

Based on the analysis above, flower buds in the length of 4–6 mm containing meiotic PMCs were collected from the heat-treated and non-heat-treated plants. For each biological replicate, 18–25 flowers were randomly taken from the tomato plants, three replicates were included for each treatment condition. Once detached from the plants, flower buds were immediately soaked in a pre-chilled fixative solution (75% ethanol and 25% acetic acid). To prepare for the LCM slides, flower buds were infiltrated under vacuum for 10 min using the following protocol: 1) wash in fresh fixative solution once; 2) wash (2 X) in phosphate buffered saline (PBS) containing 10% sucrose and protease inhibitors; 3) wash (2 X) in PBS buffer containing 20% sucrose and the same concentration of protease inhibitors. Then flower buds were imbedded in OCT compound and frozen into blocks. Frozen tissues were sectioned into 20 µm thick slices (which is approximately twice the size of the PMCs and the same size of mature pollen) using the method described previously^[22,25]. As shown in Fig. 1, the LCM slides were prepared by transferring 40–48 cross-sections of the stamen onto each pre-coated adhesive slides (5.5 cm × 2.5 cm, Fig. 1a). From each individual flower bud, 50 sections were collected. One section (each section has 6–8 stamen) was randomly picked and stained with DAPI to examine pollen developmental stages. Stamen containing the meiotic PMCs were selected; these cells were picked from the same stamen on the remaining 49 sections.

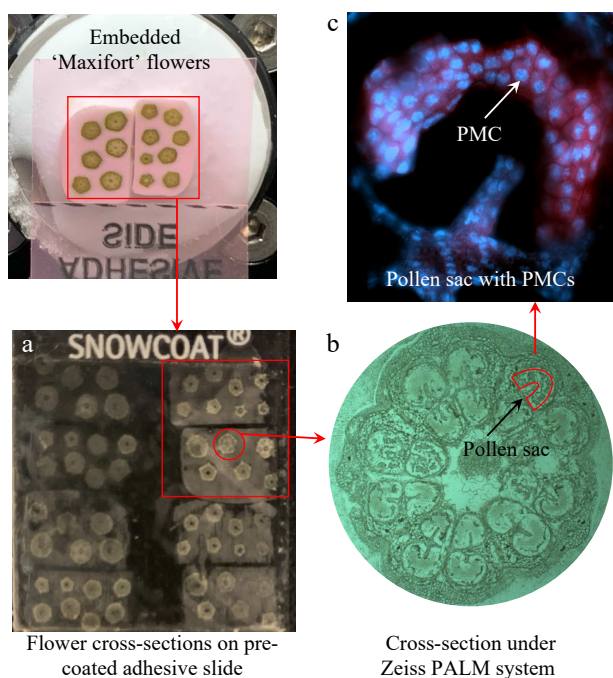


Fig. 1 Collection of pollen mother cells using laser-capture microdissection from cross-sections of frozen flower buds of tomato 'Maxifort'. (a) Transference of sectioned tissues onto a pre-coated adhesive slide; (b) flower bud cross-sections visualized under Zeiss PALM system; (c) images of DAPI stained PMCs showing the blue fluorescent nuclei.

For the collection of meiotic PMCs using LCM, the frozen slides were rinsed twice in 75% ethanol each for 1 min, and 100% ethanol for 30 s. Cells were captured by cutting the target regions in pollen sacs followed by lifting onto capture caps using the PALM MicroBeam LCM with UV laser system (Zeiss). The majority of the pollen sacs (Fig. 1b) contained the meiotic PMCs (Fig. 1c) which were separated from the other pollen sac tissues. For each biological replicate, approximately 150,000 to 200,000 cells were collected, and three replicates were harvested for both heat-treated and non-heat-treated conditions.

Protein extraction and tandem mass tag (TMT) labelling

Protein was extracted using the Pressure Cycling Technology (PCT) method developed for LCM captured cell samples with modifications^[23]. Briefly, cells captured on the collection caps were re-suspended in 35 μ L PCT buffer comprising of 20 mM 4-(2-hydroxyethyl)-1-piperazineethanesulfonic acid (HEPES), 4 M urea, 2% sodium dodecyl sulfate (SDS), and 2 mM ethylenediaminetetraacetic acid (EDTA) (Sigma, St. Louis, MO) at pH 8.0. Protein was extracted using a Barocycler 2320 EXT (Pressure Biosciences Inc., Easton, MA) which was run at 45 kPsi pressure for 60 cycles at 25 $^{\circ}$ C. The protein extracts were transferred to 1.5 mL low protein binding micro-centrifuge tubes followed by centrifugation at 10,000 g, 4 $^{\circ}$ C for 15 min. Supernatants containing proteins were transferred to fresh tubes. Protein concentration was assayed using Qubit Protein Assay kit on a Qubit 3.0 Fluorometer (Life Technologies, Carlsbad, CA).

Twenty-five μ g of protein was taken from each sample. Proteins were reduced using tris (2-carboxyethyl) phosphine (TCEP), and cysteine residues were blocked with methyl methanethiosulfonate (mM MMTS) (Sigma). Proteins were

loaded onto an S-TRAP Micro column (PROTIFI, Long Island, NY) for removal of SDS and urea. On-column trypsin digestion was performed at 35 $^{\circ}$ C for 16 h using Sequencing Grade Modified Trypsin (Promega, Madison, WI). The digested peptide samples were eluted sequentially in 50 mM triethylammonium bicarbonate (TEAB) buffer, 0.2% formic acid (FA), and finally 50% acetonitrile (ACN) in water and 0.2% FA. All elutes were combined and dried down under vacuum. Each tryptic peptide sample was reconstituted in 50 mM TEAB and labeled with TMT tags following the manufacturer's instructions (ThermoFisher Scientific, Waltham, MA). The three HS replicates were labeled with tags 127N, 129N, 130C; and the three non-HS-treated (N-HS) replicates were labeled with tag 127C, 128N, 131C. The six labeled peptide samples were pooled; unbound tags were removed using mixed-mode cation exchange procedure through 30-mg \times 30- μ m 1-mL cartridges following the manufacturer's instruction (Oasis MCX Vac; Waters, Milford, MA). Peptide samples were eluted twice in 75% ACN with 10% NH_4OH and evaporated to complete dryness under vacuum.

High pH reverse phase (hpRP) fractionation and nano-liquid chromatography and mass spectrometry analysis (LC-MS/MS)

The TMT-labeled peptide samples were reconstituted in buffer A (20 mM NH_4HCO_2 , pH 9.5 in water), and loaded onto an XTerra MS C18 Column, 125 \AA , 3.5 μ m, 150 mm \times 2.1-mm (Waters) for fractionation by eluting with a gradient (10 to 45%) buffer B containing 80% ACN with 20% 20 mM NH_4HCO_2 ^[26]. In total, 48-fractions were collected and pooled into 12 fractions with a multiple fraction concatenation strategy. All 12 fractions were dried and reconstituted in 2% ACN with 0.5% FA for nanoLC-MS/MS analysis^[27].

The nano LC-MS/MS was carried out using an Orbitrap Fusion mass spectrometer (Thermo-Fisher Scientific) equipped with nano ion source using high energy collision dissociation (HCD)^[28]. The Orbitrap Fusion was coupled with an UltiMate 3000 RSLCnano (Dionex; ThermoFisher Scientific). Each reconstituted fraction was injected into a PepMap C-18 RP nano trap column (3 μ m, 75 μ m \times 20 mm) (Dionex) for on-line desalting and then into a PepMap C-18 RP column (3 μ m, 75 μ m \times 15 cm) for peptide separation. The Orbitrap Fusion was operated in positive ion mode. The instrument was operated in data-dependent acquisition (DDA) mode using the Fourier transform (FT) mass analyzer to conduct survey MS scans for selecting precursor ions, followed by 3 s, top speed, data-dependent HCD-MS/MS scans of precursor ions with between 2–7 positive charges and threshold ion counts of > 10,000. The normalized collision energy was 37.5%. MS survey scans were conducted at a resolving power of 120,000 full width at half maximum (fwhm) at m/z 200, for the mass range of m/z 400–1600 with AGC and Max IT settings of 3e5 and 50 ms, respectively. MS/MS scans were conducted at a resolution of 50,000 fwhm for the mass range m/z 105–2000 with AGC and Max IT settings of 1e5 and 120 ms. The Q isolation window was set at \pm 1.6 Da. Dynamic exclusion duration was set at 60 s with a repeat count of 1, a 50 s repeat duration and a \pm 10 ppm exclusion mass width. All data was acquired under Xcalibur 3.0 operation software and Orbitrap Fusion Tune 2.0 (Thermo-Fisher Scientific).

The MS and MS/MS raw spectra from all the six labeled samples were processed and searched using Sequest HT software within Proteome Discoverer 2.2 (ThermoFisher Scientific). Tomato protein version ITAG2.40 was used as searching

database. Identified peptides were filtered using the Percolator algorithm in PD 2.2 with a maximum 0.05 false discovery rate (FDR), and high peptide confidence. Quantifiable spectra were assigned to peptide spectra detected with all reporter ions.

Identification of the quantified proteomes and differentially expressed proteins in heat stress (HS)-treated pollen mother cells

Proteins were filtered for those being assigned with two or more unique peptides in the PD 2.2 report. The normalized abundance values of reporter ions from the TMT tags (representing the protein abundances in labeled samples) were used to calculate the ratio value between HS and N-HS conditions for each protein and then subjected to Log_2 transformation. The log_2 ratio (HS/N-HS) values (hereafter named as fold (HS/N-HS)) were fit into a normal distribution to obtain the standard deviation (SD) using SAS (Version 9.3; SAS Institute, Cary, NC)^[29,30]. The fold (HS/N-HS) datasets (three replicates for each treatment condition) were subjected to t-test to generate the raw P followed by FDR correction using SAS. The HS regulated differentially expressed proteins (HS-DEPs) were selected using the following criteria: fold (HS/N-HS) passing the cut-off threshold at greater than $2 \times \text{SD}$ (\pm) and an FDR adjusted $P \leq 0.05$ ^[22,31]. The HS-up-regulated DEPs have a fold change greater than 0 (positive value), and down-regulated proteins have a fold change less than 0 (negative value).

Analysis of heat stress regulated differentially expressed proteins (HS-DEPs) and heat tolerance of pollen mother cells

The HS-DEPs were analyzed for Gene Ontology (GO) categories using Plant MetGenMap^[32]. Protein–protein interaction networks were constructed using STRING with medium confidence set at 0.400, and the Markov cluster (MCL) algorithm at an inflation parameter of 3^[33]. Protein–protein association network integrating with fold (HS/N-HS) was visualized in Cytoscape 3.7.1^[34]. Additional literature searches were used to identify the roles of DEPs individually as well as functional groups in affecting PMCs development under HS condition.

RESULTS AND DISCUSSION

The correlation between the size of tomato flower buds and pollen development stages

The 11 flower buds on a tomato 'Maxifort' flower cluster ranging 3–12 mm in length were divided into three groups (Fig. 2). The cross-sections of these flower buds were stained with DAPI to observe the pollen developmental stages under a microscope. Nine distinct pollen developmental stages were identified with the sizes of corresponding flower buds (stamen length) (Table 1). Based on this analysis, tomato flower buds in group 1 with 4–6 mm long stamen should contain PMCs at premeiotic, meiosis I and II stages.

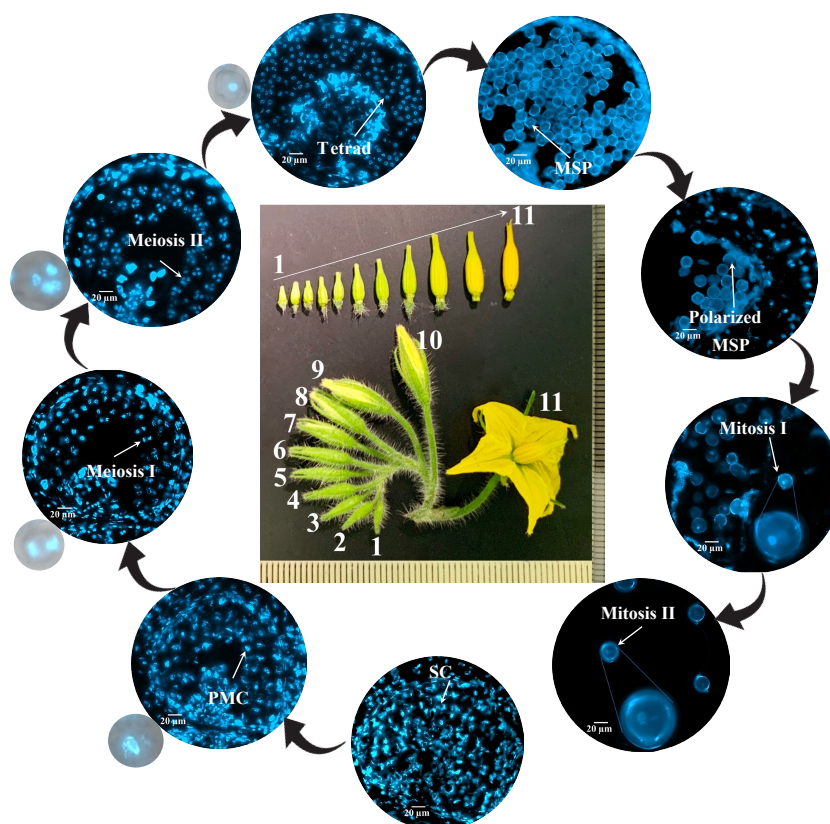


Fig. 2 Correlation between flower size and male gametophyte development stages in tomato 'Maxifort'. Frozen cross section of tomato 'Maxifort' flower buds were stained with 4',6-diamidino-2-phenylindole (DAPI). Images were taken under an upright Zeiss imager M2 with EC PlnN 40X objective and a BP335-383 excitation DAPI filter. The inflorescence of 'Maxifort' flower were labeled 1–11. Nine distinct developmental stages were identified including: 1) sporogenous cells (SC); 2) pollen mother cells (PMCs); 3) meiosis I to dyads; 4) meiosis II to tetrads; 5) tetrads to early microspore; 6) microspore (MSP); 7) polarized MSPs; 8) mitosis I; 9) mitosis II. Zoom-in image of PMCs, meiosis I, meiosis II and tetrads with merged bright field and DAPI channel are displayed to show pollen cell structure.

Table 1. The correlation between flower size and pollen developmental stages

Flower size (stamen length mm)	Pollen developmental stage	Note
Flower size 1–6 (3–6 mm)	Sporogenous cells (SCs), Pollen mother cells (PMCs), Meiosis I to dyads, Meiosis II to tetrads, Tetrads to early microspores	Microsporogenesis: PMCs undergo meiosis I and II to produce haploid tetrad.
Flower size 7–8 (7–9 mm)	Microspores (MSPs), Polarized MSPs	Unicellular microspores release, and polarization.
Flower size 9–11 (9–12 mm)	Mitosis I, Mitosis II	Microgametogenesis: Microspores undergo mitosis I and II to produce pollen grain.

Quantitative proteomics analysis and identification of HS-regulated differentially expressed proteins (HS-DEPs)

Using LCM method, approximately 150,000–200,000 PMCs were collected and subjected for proteome profiling. From the meiotic PMCs samples, a total of 8,569 proteins were identified, of which 6,343 proteins were quantified with two or more unique peptides (Supplemental Table S1). Among these quantified proteins, the number of proteins decreased with increasing number of peptides assigned to a protein (Fig. 3a). The values of fold (HS/N-HS) of quantified proteins fit to a normal distribution with the population mean at 0 and SD at 0.3. When the quantified proteome was divided into three groups based on the fold (HS/N-HS) using the ± 0.30 as a cut-off value, 749 proteins were in the range from -1.64 to -0.29 (HS-down-regulated proteins), 4,955 proteins in the range from ± 0.30 (non-changed proteins), 729 proteins in the range from 0.31 – 2.40 (HS-up-regulated proteins) (Fig. 3b). The quantified proteins then were filtered using fold (HS/N-HS) ≥ 0.60 or ≤ -0.60 , and FDR adjusted $P \leq 0.05$, which gives 95% confidence

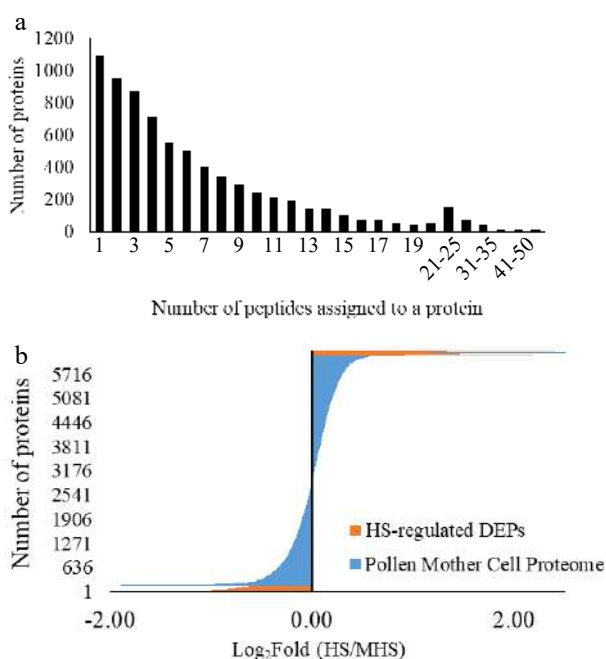


Fig. 3 Protein distribution in the quantified proteomes from pollen mother cells of tomato 'Maxifort'. (a) Protein distribution based on the number of unique peptides assigned to each protein; (b) protein distribution based on the fold change from HS to N-HS conditions. HS-regulated proteins: the number and fold distribution of proteins showing significant differences in abundance level from HS-treated to non-HS-treated conditions; Pollen mother cell proteome: the quantified proteome with two or more peptides assigned to the identified protein from the HS-treated and non-HS-treated groups.

for the selection of HS-DEPs. Of the quantified proteins, 4% (254 proteins) are DEPs comprising 96 HS-up-regulated DEPs (13% of the 729 HS-up-regulated proteins) and 158 HS-down-regulated DEPs (21% of 749 HS-down-regulated proteins) (Supplemental Table S2).

Functional categories of HS-regulated DEPs

The enriched GO terms of the HS-regulated DEPs were searched against the tomato genome using the multi-test correction FDR ($P < 0.05$) in Plant MetGenMap. When enriched based on functions, the HS-up-regulated DEPs were clustered into four groups including protein binding, unfolded protein binding, heat shock protein (HSP) binding, and chaperone binding. The HS-down-regulated DEPs were enriched into four groups, with functions in regulating enzyme activities (Fig. 4a). When searched for biological processes, the 158 HS-down-regulated DEPs only formed a single carbohydrate metabolism group, whereas the 96 HS-up-regulated DEPs were enriched into a number of GO terms including RNA processing, translation, transcription, protein folding, targeting, responses to stress, mitotic spindle organization, male gamete generation and heat acclimation (Fig. 4b, Supplemental Table S3). These results indicate that the HS-up-regulated DEPs, although with a smaller number of proteins, affected a broader range of biological processes than the HS-down-regulated DEPs.

When the HS-regulated DEPs were analyzed for functional classification using MetGenMap, 11 functional groups (GO terms) were identified (Fig. 5, Supplemental Table S4). The largest functional group is protein binding, which contained 104 proteins (out of the 254 DEPs). In this group, 55 proteins were HS-down-regulated proteins, and 49 proteins were HS-up-regulated proteins. The majority of HS-up-regulated proteins are HSPs which bind to other proteins with a primary function as chaperones. The outer membrane lipoprotein blc (Solyc07g005210.2.1, 1.86 fold) showed the highest increase in HS-treated PMCs. This protein is involved in the storage or transport of lipids necessary for membrane maintenance under stress conditions^[35]. This is the first report that this protein was found to be accumulated in PMCs under HS conditions, it may indicate a significant role in protecting membrane systems from heat-induced damage. Proteins from multiple member families such as peptidyl-prolyl cis-trans isomerases, Bax inhibitors, and serine/threonine protein kinases have separate isoforms as either HS-down- or up-regulated proteins. In the transcription factor activity group, the heat stress transcription factor A3 (*HSFA3*) had the highest increase in abundance level under HS condition (Solyc08g062960.2.1, 1.12-fold). HSFs specifically bind to the palindromic heat shock elements (HSEs: 5'-AGAAnnTTCT-3') conserved in promoters of HS-inducible genes such as those encoding for HSPs, these proteins (genes) are known as master regulators for induced thermo-tolerance in tomato^[36–38]. In tomato pollen, compared to *HSFA1* as a master regulator, *HSFA3* was observed strongly induced under

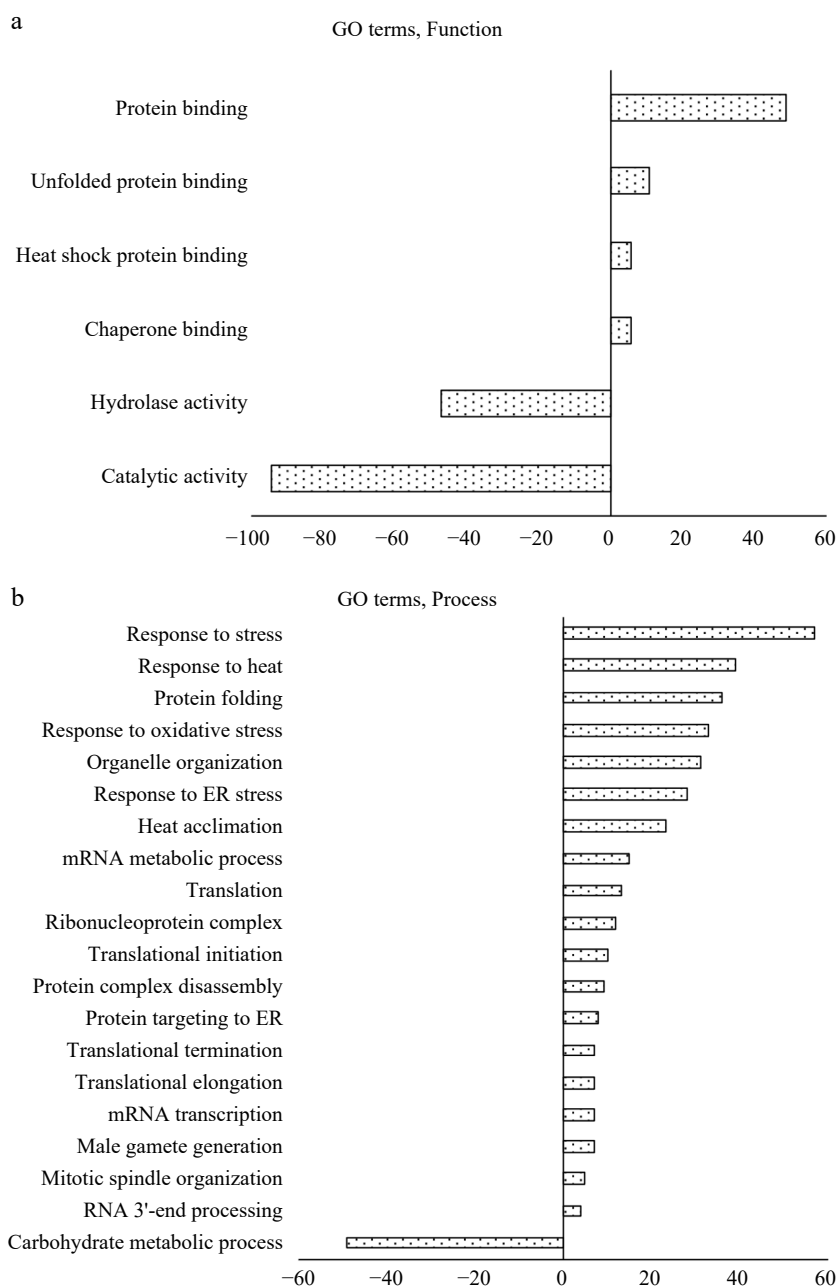


Fig. 4 Enrichment gene ontology (GO) analysis of heat stress regulated DEPs (HS-DEPs) in pollen mother cells (PMCs), which include 158 DEPs-down-regulated protein and 96 DEPs-up-regulated proteins. (a) GO terms of molecular functions; (b) GO terms of biological processes. Positive value indicates HS-up-regulated DEPs and negative value indicates HS-down-regulated DEPs. The classification analysis was conducted using multivariate test at FDR adjusted $P \leq 0.05$ in Plant MetGenMap (<http://bioinfo.bti.cornell.edu/cgi-bin/MetGenMAP/home.cgi>).

HS and regulates subsets of heat stress related genes in a tissue-specific manner^[39]. This is consistent with our proteome analysis, in which expression level of *HSFA1* (Solyc08g005170) was not changed, while *HSFA3* was significantly up-regulated. Overexpression of *Arabidopsis HSFA3* in the quadruple *HSFA1a/b/d/e* knockout mutant can restore thermo-tolerance, indicating this gene regulates plant heat stress responses independently from the master HSFs^[40]. Concurrently, the *Arabidopsis* mutant lacking *HSFA3* expression showed a decreased expression in HS resistant proteins and was more sensitive to prolonged heat stress^[41,42]. A recent study shows that these HSFs are also involved in epigenetic mechanisms for HS tolerance^[37]. In this study, the HS-up-regulated changes in the

tomato *HSFA3* and HSPs at the protein level clearly confirmed the important role of these proteins in tolerance to momentary as well as intermittent HS of PMCs as in the case of temperature fluctuation during the summer season.

Protein-protein association networks

The 254 HS-regulated DEPs were submitted to STRING database; 139 proteins were placed in 31 clusters (Supplemental Table S5) based on their physical and functional associations (25 major clusters are listed in Table 2). The protein-protein interactions were higher than the expected value at a protein and protein interactions (PPI) enrichment P-value of 3.22×10^{-15} , which indicates that proteins clustered together are not

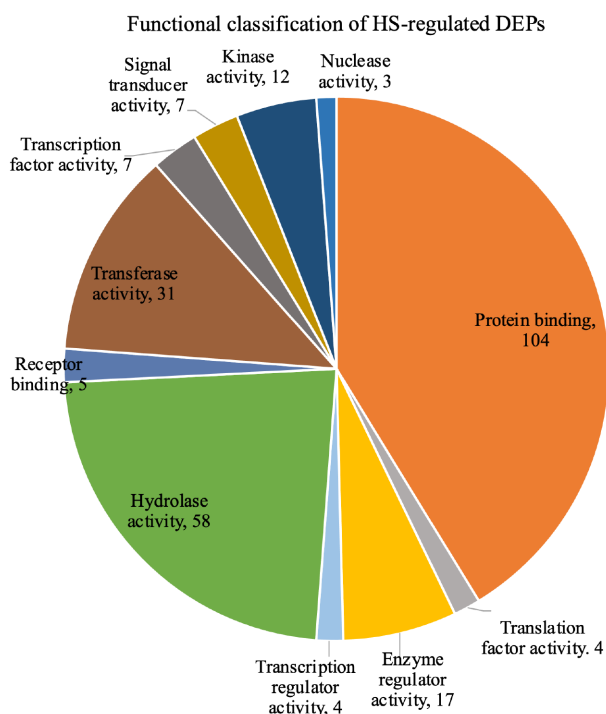


Fig. 5 Pie chart of functional groups enriched with DEPs using Plant MetGenMap. Some proteins were placed in more than one functional group. GO terms are: Nuclease activity (GO:0004518); Protein binding (GO:0005515); Translation factor activity (GO:0008135); Enzyme regulator activity (GO:0030234); Transcription regulator activity (GO:0030528); Hydrolase activity (GO:0016787); Receptor binding (GO:0005102); Transferase activity (GO:0016740); Transcription factor activity (GO:0003700); Signal transducer activity (GO:0004871); Kinase activity (GO:0016301).

random events^[23,43]. Most of the clusters (except for clusters 14, 16, 19) were connected with each other directly or indirectly; this suggests a systemic change of proteomes leading to extensive reorganization of molecular and cellular processes in PMCs under the HS condition (Fig. 6).

Under HS conditions, the accumulation of unfolded proteins in the cytosol activates the cytosolic heat stress responses (HSRs) inducing the expression of heat shock factors (HSFs) and heat shock proteins (HSPs)^[44,45]. Clusters 1, 3, 4, 17, 18 contained a large number of HS-up-regulated HSPs associated with various molecular processes. These HSPs play an irreplaceable role in ameliorating cytosolic HS through mediating the process of folding, refolding, re-solubilization of protein aggregates and removal of damaged peptides and proteins^[19,46–48]. Data from these clusters clearly indicated that HSPs provided the major protection mechanisms for the PMCs under HS condition. The increases in these HSPs concurred with previous research where HSPs and HSFs showed a higher expression level in heat-tolerant than heat-sensitive tomato varieties^[49,50]. The ubiquitin-mediated degradation of intracellular proteins in cluster 9; and peptide methionine sulfoxide reductase, thioredoxins in cluster 12 for protecting cells against oxidative damage were all down-regulated. Furthermore, in cluster 7, the prolyl oligopeptidase family protein (protein #28, -0.68 -fold) which is involved in the maturation and degradation of peptide hormones^[51] was down-regulated, whereas synaptobrevin (protein #53, 1.28 -fold) with a sort-and-degrade mechanism for damaged proteins was up-regulated.

In cluster 1, in addition to the HSPs, the calreticulin (coordinating protein targeting on ER) and ethylene-responsive transcriptional coactivator were HS-up-regulated. The ethylene-responsive transcriptional coactivator is required for the ethylene-response pathways which are important thermo-tolerance mechanisms in tomato^[52]. The peptidyl-prolyl cis-trans isomerase (PPI, protein #1) and S-adenosylmethionine synthase (protein #116) are also involved in protein folding/targeting via different mechanisms, these proteins were HS-down-regulated.

The PPI in cluster 1 was connected to the superoxide dismutase (protein #9) in cluster 2 because of commonality in functions, and with the tetratricopeptide repeat protein (TPR) 2-like (protein #93) in cluster 12 because PPIs also contain the TPR domain. Cluster 2 is comprised of nine ribosomal proteins (up-regulated) and five TPR (down-regulated). The TPR protein family has been shown to be involved in a diverse spectrum of cellular functions including protein transport, and protein folding, modulation of eukaryotic translation through the interaction with DDX3 RNA helicase^[53]. The ribosomal proteins were interconnected with cluster 6, in which proteins for transcription and translation were all down-regulated in HS-treated PMCs. Through connections of proteins #89-#66-#86, cluster 2 was associated with cluster 15 which contained the down-regulated TFs and signaling pathways. Cluster 8 contained proteins affecting chromatin status. The histone subunit proteins were up-regulated, the proteins for the transcriptional status (DNA-binding protein, protein #112, -1.44 -fold; nucleosome assembly protein, protein #113, -0.69 -fold) were down-regulated, indicating a repressed transcriptional activity. Taking these three clusters together, the higher abundance level of the ribosomal proteins might indicate a more resilient thermo-stability of these ribosomal proteins, not necessarily correlated with de novo protein biosynthesis.

Proteins in clusters 4 and 13 are related to cytosolic heat stress response/programmed cell death. In cluster 4, the nine proteins were all up-regulated. The Bcl-2-associated athanogene (protein #120, 1.04 fold) is a membrane protein that blocks a step in a pathway leading to apoptosis or programmed cell death. In cluster 13, the VASCULAR-RELATED NAC-DOMAIN 6 (protein #58) regulating programmed cell death was up-regulated^[54]. Two proteins annotated to Importins (protein #98, 99) which importing proteins from cytoplasm into nucleus were both down-regulated.

In cluster 18, the 3-ketoacyl-CoA thiolase (protein #92) catalyzes the last step of the mitochondrial beta-oxidation pathway, it has a role in abolishing BNIP3-mediated apoptosis and mitochondrial damage^[55]. Similarly, in cluster 24, a phosphosulfolactate synthase-related protein (protein #24) was up-regulated. A study on *A. thaliana* showed that the HS-associated 32-kD protein (*Hsa32*), which is a phosphosulfolactate synthase-related heat-shock protein, is required for the maintenance of acquired thermo-tolerance^[56].

Clusters 3, 16, 17, 25 comprised proteins related to cell wall properties including cellulase and laccase, and proteins affecting degradation and elasticity of cell walls. These proteins were all down-regulated. Additionally, cluster 20 contained pectin lyase-like superfamily protein (protein #51, -1.3 -fold) and meiotic serine proteinase (protein #128, -1.14 -fold), which catalyzes cell surface proteolysis for PMCs to proceed to

Table 2. Proteins clustered on STRING association networks^z

Cluster number ^y	Protein # ^x	Protein accession ^v	Protein description ^u	Fold change ^w
Cluster 1: Protein folding/ unfolding/ targeting	1	Solyc06g051650.2.1	Peptidyl-prolyl cis-trans isomerase	-0.60
	3	Solyc05g056230.2.1	Calreticulin	0.8
	8	Solyc01g104740.2.1	Ethylene-responsive transcriptional coactivator	0.7
	14	Solyc06g076520.1.1	HSP20	1.11
	15	Solyc03g082420.2.1	Small heat shock protein	1.05
	16	Solyc11g020040.1.1	HSP 70	0.96
	18	Solyc02g088610.2.1	ClpA/Clp HSP	0.78
	29	Solyc01g086740.2.1	Chaperone DnaJ	0.6
	36	Solyc01g099660.2.1	HSP 70	0.67
	54	Solyc02g077670.2.1	Chaperone protein dnaJ 2	1.41
	96	Solyc11g006170.1.1	DnaJ	0.62
	100	Solyc11g071830.1.1	Chaperone protein dnaJ	1.36
	109	Solyc07g053620.2.1	Chaperone protein dnaJ	0.63
	115	Solyc03g005700.1.1	Mitochondrial import receptor subunit TOM22	0.67
116	Solyc10g083970.1.1	S-adenosylmethionine synthase	-0.60	
Cluster 2: Protein translation	9	Solyc06g048410.2.1	Superoxide dismutase	0.64
	31	Solyc01g094560.2.1	Eukaryotic ribosomal protein eL36 family	0.79
	35	Solyc01g097760.2.1	Ribosomal protein L7a	0.63
	39	Solyc01g103510.2.1	Ribosomal protein L3 family	0.91
	45	Solyc02g038650.1.1	Tetratricopeptide repeat protein 5	-1.15
	46	Solyc02g038660.1.1	Tetratricopeptide-like helical	-0.64
	47	Solyc02g038670.1.1	Tetratricopeptide-like helical	-0.83
	48	Solyc02g038680.1.1	Tetratricopeptide-like helical	-1.04
	49	Solyc02g038700.1.1	Tetratricopeptide repeat protein 5	-1.00
	61	Solyc03g112360.1.1	Ribosomal protein	0.61
	82	Solyc06g064460.2.1	Ribosomal protein L7a	0.64
	94	Solyc10g061970.1.1	60S ribosomal protein L37a	0.63
	126	Solyc10g085480.1.1	60S ribosomal protein L24	0.66
	132	Solyc05g008420.2.1	Tetratricopeptide repeat protein 5	-0.62
Cluster 3: Defense against cell wall stress factors	5	Solyc04g072160.2.1	Prostaglandin E synthase 3	0.78
	33	Solyc01g095320.2.1	BCL-2-associated athanogene 6	0.91
	50	Solyc02g065170.2.1	Laccase-22	-0.61
	66	Solyc03g117630.1.1	HSP70	1.02
	67	Solyc03g118430.2.1	Peptidase family M16	-0.74
	74	Solyc04g014480.2.1	HSP20-like chaperones	1.29
	79	Solyc05g056560.2.1	C11orf73 homolog	0.95
	80	Solyc06g053380.2.1	Chitinase	-1.11
	87	Solyc07g005820.2.1	Heat shock protein	0.89
	91	Solyc09g075950.1.1	Heat shock protein 70 family.	1.35
	103	Solyc09g092690.2.1	Peptidyl-prolyl cis-trans isomerase	1.27
107	Solyc10g007220.1.1	Hsp40, DnaJ	-1.05	
Cluster 4: Cytosolic heat stress response/ programmed cell death	13	Solyc08g062340.2.1	Cytosolic class II small heat shock protein HCT2	1.56
	21	Solyc08g062450.1.1	Class II small heat shock protein Le-HSP17.6	1.09
	22	Solyc08g078700.2.1	HSP20	1.38
	37	Solyc01g102960.2.1	HSP20	1.3
	62	Solyc03g113930.1.1	HSP20	1.29
	90	Solyc09g015000.2.1	HSP20	1.86
	64	Solyc03g115230.2.1	ClpA/ClpB HSP	0.61
	120	Solyc10g084170.1.1	Bcl-2-associated athanogene	1.04
133	Solyc09g015020.1.1	Small heat shock protein (HSP20)	1.91	
Cluster 5: Rerouting the carbohydrate flux	6	Solyc04g082200.2.1	Bcl-2-associated athanogene	1.37
	30	Solyc01g091200.2.1	NAD dependent epimerase/ dehydratase	-0.79
	44	Solyc01g112210.2.1	Hexosyltransferase	-0.61
	68	Solyc03g120310.2.1	Glycosyl transferase	-0.99
	77	Solyc05g054060.2.1	UTP-glucose 1 phosphate uridylyltransferase	-0.65
	125	Solyc06g074670.2.1	NAD-dependent epimerase/ dehydratase	-0.76
	88	Solyc07g055300.2.1	Alpha alpha-trehalose-phosphate synthase	-0.62
119	Solyc07g007790.2.1	Sucrose phosphate synthase	0.6	
Cluster 6: Transcription/ translation	11	Solyc10g051390.1.1	RNA-binding glycine-rich protein-1b	-0.99
	59	Solyc03g059010.2.1	Glucose-repressible alcohol dehydrogenase transcriptional effector CCR4	-0.83

(to be continued)

Table 2. (continued)

Cluster number ^y	Protein # ^x	Protein accession ^y	Protein description ^u	Fold change ^w
	75	Solyc04g074750.2.1	RNA-binding (RRM/RBD/RNP motifs)	-0.60
	78	Solyc05g054240.2.1	Protein arginine N-methyltransferase	-0.64
	81	Solyc06g062800.2.1	DEAD box helicase family	0.63
	84	Solyc06g071560.2.1	Phosphatase 2A regulatory subunit B	-1.45
	89	Solyc09g008620.1.1	Polyadenylate-binding protein	-1.14
Cluster 7: Cytosolic protein degradation and secretion	28	Solyc01g079450.2.1	Prolyl oligopeptidase family protein	-0.68
	40	Solyc01g105990.2.1	Os01g0107900 protein	-0.64
	53	Solyc02g069160.2.1	Synaptobrevin family	1.28
	83	Solyc06g071430.2.1	T17H3.1 protein	-0.74
	111	Solyc11g066830.1.1	Splicing factor U2af subunit	0.66
Cluster 8: Chromatin status/ gene transcriptional activity	12	Solyc06g074790.1.1	Histone H2B.1	0.71
	17	Solyc01g099410.2.1	Histone H2A.1	0.61
	112	Solyc03g116770.2.1	DNA-binding protein	-1.44
	113	Solyc06g062690.2.1	Nucleosome assembly protein	-0.69
	114	Solyc11g066160.1.1	Histone H4	0.65
Cluster 9: Ubiquitin-mediated degradation of intracellular proteins	4	Solyc09g074680.2.1	Cullin family	-0.63
	43	Solyc01g111680.2.1	Ubiquitin-conjugating enzyme	-0.61
	104	Solyc05g052960.2.1	BTB/POZ domain containing protein	-0.72
	105	Solyc06g073820.1.1	Ubiquitin carboxyl-terminal hydrolase	-1.10
	106	Solyc11g072070.1.1	BTB/POZ domain containing protein	-0.63
Cluster 10: Synthesis of secondary metabolites	26	Solyc01g010900.2.1	Cytochrome P450	-0.78
	123	Solyc03g053130.2.1	Calcium-dependent phosphotriesterase	-0.96
	122	Solyc07g065770.2.1	ABC transporter-like	-0.85
	124	Solyc11g071800.1.1	Strictosidine synthase	-0.68
Cluster 11: Stress-response	20	Solyc09g065180.2.1	mRNA binding protein	-0.80
	25	Solyc06g076570.1.1	HSP20	2.4
	63	Solyc03g114930.2.1	PsbP-like protein 1	-0.67
	118	Solyc08g080190.2.1	Glucose-methanol-choline (GMC) oxidoreductase	-0.99
Cluster 12: Protecting cells against oxidative damage	7	Solyc03g111720.2.1	Peptide methionine sulfoxide reductase	-1.02
	72	Solyc04g010010.1.1	Thioredoxin-like protein 1	-1.05
	73	Solyc04g010030.1.1	Thioredoxin-like protein 1	-1.32
	93	Solyc10g007230.1.1	Tetratricopeptide repeat protein 2-like	-1.64
Cluster 13: Programmed cell death/ protein targeting	38	Solyc01g103080.2.1	RNA helicase, ATP-dependent	1.15
	58	Solyc03g025740.2.1	VASCULAR-RELATED NAC-DOMAIN 6	0.64
	98	Solyc11g011790.1.1	Importin beta-3	-1.09
	99	Solyc11g011800.1.1	Importin beta	-0.90
Cluster 14: Lipidome	10	Solyc08g076470.2.1	Glycerol-3-phosphate acyltransferase	-0.76
	32	Solyc01g094700.2.1	Glycerol-3-phosphate acyltransferase	-0.81
	42	Solyc01g109580.2.1	Adenylyl cyclase-associated protein	-0.74
	110	Solyc07g005580.2.1	Phospholipid/glycerol acyltransferase	-0.75
Cluster 15: TFs and signaling pathways	27	Solyc01g057270.2.1	Calmodulin-binding transcription factor SR4	-0.95
	86	Solyc06g083150.2.1	U-box domain-containing protein	-0.82
	137	Solyc07g055130.2.1	Kinase family protein	-0.75
Cluster 16: Cell Wall degradation/ PMC separation	34	Solyc01g097000.2.1	Glycosyl hydrolase family protein	-0.77
	85	Solyc06g073750.2.1	Beta-D-glucosidase	-0.80
	127	Solyc11g071640.1.1	Beta-D-glucosidase	-0.65
Cluster 17: Elasticity of cell surface structures	70	Solyc03g123540.2.1	HSP20-like chaperones	1.78
	101	Solyc09g092160.2.1	Beta-galactosidase	-0.76
	108	Solyc05g014280.2.1	Small heat shock protein	1.59
Cluster 18: Attenuating the apoptotic effects and mitochondrial damages	102	Solyc11g020330.1.1	Small heat shock protein	2.18
	41	Solyc01g106820.2.1	Peptidase M50 family	1.1
	92	Solyc09g091470.2.1	3-ketoacyl CoA thiolase 2	0.68
Cluster 19: Meiotic process	57	Solyc03g007800.2.1	Topoisomerase 1-associated factor 1/Timeless family protein	0.7
	71	Solyc04g008600.2.1	Chromosome segregation in meiosis protein 3	0.7
	136	Solyc11g020780.1.1	DCK/dGK-like deoxyribonucleoside kinase	-0.60
Cluster 20: Cell surface activities on premeiotic PMCs affecting fate of the cells	51	Solyc02g068400.2.1	Pectin lyase-like superfamily protein	-1.31

(to be continued)

Table 2. (continued)

Cluster number ^y	Protein # ^x	Protein accession ^y	Protein description ^u	Fold change ^w
Cluster 21: N/A	128	Solyc08g077860.2.1	Meiotic serine proteinase	-1.14
	23	Solyc07g054210.2.1	Protochlorophyllide reductase like protein	-0.92
	121	Solyc10g008740.2.1	Mg-protoporphyrin IX chelatase-like	-0.62
Cluster 22: Folding and targeting of nascent proteins	52	Solyc02g069120.2.1	Zinc-finger protein ZPR1	0.61
	56	Solyc02g090480.2.1	Peptidyl-prolyl cis-trans isomerase D	-0.61
Cluster 23: Pre-meiotic chromosome	69	Solyc03g120900.1.1	Belongs to the WD repeat SEC13 family	-0.64
	135	Solyc10g007680.2.1	Regulator of chromosome condensation	-0.64
Cluster 24: Maintenance of acquired thermos-tolerance	2	Solyc08g077980.2.1	Bax inhibitor; Belongs to the B11 family	0.64
	24	Solyc02g079930.2.1	Phosphosulfolactate synthase-related protein	0.66
Cluster 25: Cell wall	95	Solyc11g005490.1.1	Fasciclin-like arabinogalactan family protein	-1.12
	138	Solyc12g013900.1.1	CT099	0.61

^z Proteins clustered on the STRING networks in Fig. 6. These proteins were identified as differentially expressed proteins (DEPs) in the heat stress (HS)-treated pollen mother cells which were significantly up-regulated or down-regulated compared to the non-HS-treated control condition. The relative difference in abundance of each protein, measured by the intensity of its constituent peptides, was compared between the two treatment conditions. The protein has passed the t test with false discovery rate (FDR) corrections ($P \leq 0.05$) and with a fold change greater than 0.60-fold (\pm). Statistical analyses were performed using SAS (Version 9.3; SAS Institute, Cary, NC)

^y Cluster number in Fig. 6, which were constructed in STRING protein-protein interaction networks using Markov cluster (MCL) algorithm

^x Protein # in Fig. 6

^w Protein accession number in the ITAG Protein database (version 2.40; Sol Genomics Network, Boyce Thompson Institute, Ithaca, NY).

^u Protein description in the ITAG Protein database (version 2.40; Sol Genomics Network, Boyce Thompson Institute, Ithaca, NY)

^u The fold (HS/N-HS) for each protein is the \log_2 ratio of the protein abundance level between heat stress (HS) and non-HS-treated (N-HS) conditions

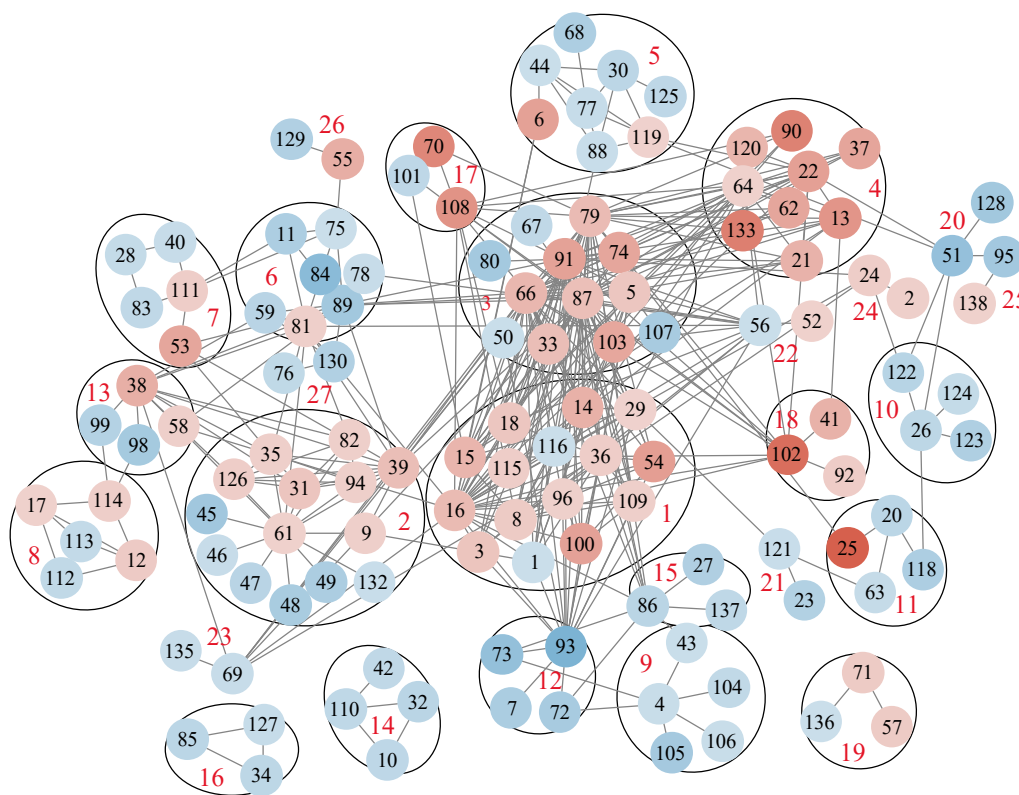


Fig. 6 Protein interaction networks of proteins showing significant change from heat stress (HS) to non-heat stress (N-HS) conditions in pollen mother cells from tomato 'Maxifort'. The network was constructed based on functional and physical interactions at medium confidence (0.400) level in STRING (<https://string-db.org>). String clusters, protein accession, and fold change are listed in Table 2. The image was generated using Cytoscope associated with the STRING database. The red color nodes are HS-up-regulated proteins, and the blue color nodes are HS-down-regulated proteins. The color depth corresponds to the protein Fold (HS/N-HS) values.

meiosis^[57]. In cluster 17, beta-galactosidase plays a functional role in the formation of extracellular elastic fibers in mammalian cells^[58], the enzyme may have similar function in affecting the surface elasticity of PMCs which will help withstand the HS induced physical dehydration in these cells.

Proteins in clusters 5, 10, 14 are involved in several metabolic pathways with proteins all down-regulated except the sucrose phosphate synthase in cluster 5. Heat stress can disrupt carbohydrate and energy metabolism resulting in a decrease of stored starch and soluble sugars in mature pollen grains and

Proteome study of tomato pollen mother cell

has an adverse impact on pollen viability^[59,60]. Cluster 5 contained seven enzymes that would change the carbohydrate flux in PMCs. The sucrose phosphate synthase catalyzes the reaction for biosynthesis of sucrose. An isoform of sucrose phosphate synthase (SPS) in rice, *OsSPS1*, was found to be essential for producing fertile pollen as well as pollen germination^[61]. Trehalose biosynthesis could be reduced due to the down-regulation in three enzymes: hexosyltransferase, UTP-glucose 1 phosphate uridylyltransferase and alpha alpha-trehalose-phosphate synthase. Trehalose was suggested to be a glycan which can serve as a replacement for water molecules around the proteins to protect them from denaturation and thus confer thermo-tolerance in pollen cells^[62]. Cluster 10 was formed by proteins for metabolism of secondary metabolites, comprising the calcium-dependent phosphotriesterase for the degradation of toxic phosphotriesters, and strictosidine synthase as a key enzyme in alkaloid biosynthesis. Cluster 14 contains three isoforms of glycerol-3-phosphate acyltransferase which is the rate-limiting enzyme in the *de novo* pathway of glycerolipid synthesis, changes in these proteins could affect lipidomes^[63].

Proteins affecting meiotic process of PMCs

Meiosis represents the earliest stage for PMCs to succumb to HS thus aborting the pollen developmental process, or to acquire thermo-tolerance and develop healthy pollen grains^[18,64,65]. Thus, we further examined the proteins enriched in GO term for male gamete generation (Supplemental Table S3) identified in the Plant MetGenMap enrichment analysis. This group was enriched with the following seven proteins: Bax inhibitor (Soly08g077980.2.1, 0.64-fold), calreticulin 2 calcium-binding protein (Soly05g056230.2.1, -0.80-fold); HSPs (Soly07g005820.2.1, 0.89-fold; Soly03g117630.1.1, 1.02-fold); two chaperone proteins (Soly11g071830.1.1, 1.36-fold; Soly02g077670.2.1, 1.41-fold), and a RNA-binding protein (Soly02g082270.2.1, 1.16-fold). The *Bax* is an apoptotic factor protein that will sense persistent meiotic defects, and then cause an arrest of meiotic processes and termination of developmental progression of the male gametes^[66]. The expression of *Bax* inhibitor suppresses *Bax*-induced cell death^[67]. In previous research, a *Bl* gene was found to be strongly expressed in male flower stamen, and artificial ectopic expression of the *Bl* homologue in *Arabidopsis* was observed with abortion of microspore development^[68]. The high abundance of *Bax* inhibitor found in the HS-treated PMCs may have a role in preventing PMCs from being aborted.

The process of pollen development from PMCs to microspores involves intense protein biosynthesis and trafficking of secretory proteins through ER and Golgi apparatus^[69]. Calreticulin is a quality control chaperone that binds to misfolded glycoproteins for refolding in the ER^[70]. HSPs function as molecular chaperones to counteract protein aggregation and target misfolded proteins for degradation^[71–73]. They play essential functions to maintain protein homeostasis in the cytosol^[74]. Heat-stress affects the developmental program of pollen, including protein homeostasis^[52], and mis-folding of nascent proteins; denaturation and aggregation of proteins can have detrimental effects from single cell to multicellular organisms^[75]. The increased accumulation of the seven HSPs could comprise a mechanism to maintain proper protein folding or removal of toxic/damaged proteins in PMCs under the HS condition.

In STRING protein association analysis, topoisomerase 1-associated factor 1 (protein #57, 0.70-fold) and chromosome segregation in meiosis protein (protein #71, 0.70-fold) were clustered together (cluster 19). Both are important proteins for chromosome segregation during meiosis. The two HS-down-regulated proteins in cluster 23, WD repeat SEC13 family (protein #69, -0.64-fold) and regulator of chromosome condensation (protein #23, -0.64-fold) are involved in premeiotic chromosome activities. In cluster 20, the meiotic serine proteinase (protein #128, -1.14-fold) catalyzes cell surface proteolysis for PMCs to proceed to meiosis^[57]. The meiotic spindle formation protein *mei-1* (Soly01g100120.2.1, -0.94-fold) affects chromosome dynamics during the meiotic prophase of PMCs^[76]. The male sterility 5 family protein (Soly06g075640.1.1, -1.01-fold) is a meiosis specific protein observed with a two-fold or higher expression level in PMCs versus anther, and is required for cell cycle exit after meiosis II in *Arabidopsis*^[77].

Furthermore, two more meiotic proteins not showing significant changes were also identified (Supplemental Table S1), including the meiotic nuclear division protein 1 homologue (Soly12g008680.1.1) and meiotic recombinase *Dmc1* (Soly09g082790.2.1). The *Dmc1* is an important protein as it contributes to cross-over formation during meiosis^[78]. Cross-over recombination products are a hallmark of meiosis because they are necessary for accurate chromosome segregation, and they allow for increased genetic diversity during sexual reproduction. The meiotic nuclear division protein participates in the process that modulates the frequency, rate or extent of meiotic nuclear division for a PMC cell to form four haploid microspores. The homeostasis of these two key proteins in the HS-treated PMCs may also provide some role in the meiotic process in 'Maxifort'.

Availability of data

The mass spectrometry proteomics data are available via ProteomeXchange database (<http://proteomexchange.org/>) via accession number PXD018915 under project title 'Heat-induced proteomes in tomato pollen mother cells'.

CONCLUSIONS

In this study, a procedure for the identification of correlation between flower size and pollen developmental stages was established for tomato 'Maxifort'. Using LCM, homogenous PMCs samples were procured from flowers exposed to HS and N-HS conditions. Quantitative proteomics analysis was used to identify the HS-induced PMCs proteomes. This dataset is a very useful resource for future investigations of pollen heat stress as it will be accessible to the public provided with this publication. In HS-treated PMCs, there was a significant increase in the abundance of HSPs, proteins blocking the apoptotic pathways and proteins facilitating chromatid segregation that allow PMCs to progress through the meiotic processes and form haploid microspores. On the other hand, proteins involved in metabolic pathways, antioxidant mechanisms, ubiquitin-mediated proteolysis processes were significantly repressed. In general, proteins affecting meiotic activities showed three types of responses to the HS: up-regulated, stable/no-change, down-regulated during premeiotic and meiotic processes. These proteins with varied responses to the HS condition could form a complex mechanism to protect PMCs to complete the

meiotic process, which may explain how the 'Maxifort' flowers still produce pollen grain under this high temperature. The HS-induced significantly changed proteins, and their encoding genes can be candidates for exploring molecular mechanisms for heat tolerance in plant reproductive organs and developing strategies to sustain tomato productivity against extreme temperatures.

ACKNOWLEDGMENTS

The authors wish to thank the following: Johanna M. Dela Cruz and Carol J. Bayles of the Imaging Facility, at Cornell University for technical support in the laser capturing and imaging process; Sheng Zhang of the Proteomics and Mass Spectrometry Facility at Cornell University, Institute of Biotechnology for expert technical assistance with mass spectrometry proteomics analysis. The authors also wish to thank Dwane Adams for professional instruction in using the Zeiss microscopic imaging system. The work in this publication was supported by 1890 Institution Teaching, Research and Extension Capacity Building Grants (CBG) Program, Award No. 2018-38821-27737, 2014-02868 and the Evans-Allen Research Funds from USDA-NIFA, and USDA-ARS CRIS Project 1907-21000-036/037-00D.

Conflict of interest

The authors declare that they have no conflict of interest.

Supplementary Information accompanies this paper at (<http://www.maxapress.com/article/doi/10.48130/VR-2022-0002>)

Dates

Received 25 October 2021; Accepted 11 February 2022; Published online 24 February 2022

REFERENCES

- Food and Agriculture Organization. 2020. FAOSTAT Database for 2019. 13 Sept. 2021 www.fao.org/faostat/en/#home
- USDA-AMS (United States Department of Agriculture, Agricultural Marketing Service). 2017. Tomatoes. USDA-AMS, Washington, DC. www.agmrc.org/commodities-products/vegetables/tomatoes
- Van Ploeg D, Heuvelink E. 2005. Influence of sub-optimal temperature on tomato growth and yield: a review. *The Journal of Horticultural Science and Biotechnology* 86:652–59
- Peet MM, Willits DH, Gardner R. 1997. Response of ovule development and post-pollen production processes in male-sterile tomatoes to chronic, sub-acute high temperature stress. *Journal of Experimental Botany* 48:101–11
- Peet MM, Sato S, Gardner RG. 1998. Comparing heat stress effects on male-fertile and male-sterile tomatoes. *Plant, Cell & Environment* 21:225–31
- Alsamir M, Mahmood T, Trethowan R, Ahmad N. 2021. An overview of heat stress in tomato (*Solanum lycopersicum* L.). *Saudi Journal of Biological Sciences* 28:1654–63
- Ayankojo IT, Morgan KT. 2020. Increasing air temperatures and its effects on growth and productivity of tomato in south Florida. *Plants* 9:1245
- Sato S, Peet MM, Thomas JF. 2000. Physiological factors limit fruit set of tomato (*Lycopersicon esculentum* Mill.) under chronic, mild heat stress. *Plant, Cell & Environment* 23:719–26
- Sato S, Kamiyama M, Iwata T, Makita N, Furukawa H, et al. 2006. Moderate increase of mean daily temperature adversely affects fruit set of *Lycopersicon esculentum* by disrupting specific physiological processes in male reproductive development. *Annals of Botany* 97:731–38
- Iwahori S. 1965. High temperature injuries in tomato. IV. Development of normal flower buds and morphological abnormalities of flower buds treated with high temperature. *Journal of the Japanese Society for Horticultural Science* 34:33–41
- Iwahori S. 1966. High temperature injuries in tomato. V Fertilization and development of embryo with special reference to the abnormalities caused by high temperature. *Journal of the Japanese Society for Horticultural Science* 35:379–86
- Levy A, Rabinowitch HD, Kedar N. 1978. Morphological and physiological characters affecting flower drop and fruit set of tomatoes at high temperatures. *Euphytica* 27:211–18
- Giorno F, Wolters-Arts M, Mariani C, Rieu I. 2013. Ensuring reproduction at high temperatures: the heat stress response during anther and pollen development. *Plants* 2:489–506
- Müller F, Rieu I. 2016. Acclimation to high temperature during pollen development. *Plant Reproduction* 29:107–18
- Rieu I, Twell D, Firon N. 2017. Pollen development at high temperature: from acclimation to collapse. *Plant Physiology* 173:1967–76
- Gómez JF, Talle B, Wilson ZA. 2015. Anther and pollen development: a conserved developmental pathway. *Journal of Integrative Plant Biology* 57:876–91
- Sato S, Peet MM, Thomas JF. 2002. Determining critical pre- and post-anthesis periods and physiological processes in *Lycopersicon esculentum* Mill. exposed to moderately elevated temperatures. *Journal of Experimental Botany* 53:1187–95
- Jeong HJ, Kang JH, Zhao M, Kwon JK, Choi HS, et al. 2014. Tomato *Male sterile 10²⁵* is essential for pollen development and meiosis in anthers. *Journal of Experimental Botany* 65:6693–709
- Zamariola L, Tiang CL, De Storme N, Pawlowski W, Geelen D. 2014. Chromosome segregation in plant meiosis. *Frontiers in plant science* 5:279
- Kumar P, Edelstein M, Cardarelli M, Ferri E, Colla G. 2015. Grafting affects growth, yield, nutrient uptake, and partitioning under cadmium stress in tomato. *HortScience* 50:1654–61
- Singh H, Kumar P, Chaudhari S, Edelstein M. 2017. Tomato grafting: a global perspective. *HortScience* 52:1328–36
- Li H, Zhu Y, Rangu M, Wu X, Bhatti S, et al. 2018. Identification of heat-induced proteomes in tomato microspores using LCM-proteomics analysis. *Single Cell Biology* 7:173
- Yang S, Li H, Bhatti S, Zhou S, Yang Y, et al. 2020. The AI-induced proteomes of epidermal and outer cortical cells in root apex of cherry tomato 'LA 2710'. *Journal of proteomics* 211:103560
- Bokvaj P, Hafidh S, Honys D. 2015. Transcriptome profiling of male gametophyte development in *Nicotiana tabacum*. *Genomics data* 3:106–11
- Martin LBB, Nicolas P, Matas AJ, Shinozaki Y, Catalá C, et al. 2016. Laser microdissection of tomato fruit cell and tissue types for transcriptome profiling. *Nature Protocols* 11:2376–88
- Yang Y, Qiang X, Owsiany K, Zhang S, Thannhauser TW, et al. 2011. Evaluation of different multidimensional LC-MS/MS pipelines for isobaric tags for relative and absolute quantitation (iTRAQ)-based proteomic analysis of potato tubers in response to cold storage. *Journal of proteome research* 10:4647–60
- Chen JW, Scaria J, Mao C, Sobral B, Zhang S, et al. 2013. Proteomic comparison of historic and recently emerged hypervirulent *Clostridium difficile* strains. *Journal of proteome research* 12:1151–61
- Yang Q, Wu J, Li C, Wei Y, Sheng O, et al. 2012. Quantitative proteomic analysis reveals that antioxidation mechanisms contribute to cold tolerance in plantain (*Musa paradisiaca* L.; ANB Group) seedlings. *Molecular & Cellular Proteomics* 11:1853–69

Proteome study of tomato pollen mother cell

29. Ye Z, Sangireddy S, Okekeogbu I, Zhou S, Yu CL, et al. 2016. Drought-induced leaf proteome changes in switchgrass seedlings. *International Journal of Molecular Sciences* 17:1251
30. Zhou S, Palmer M, Zhou J, Bhatti S, Howe KJ, et al. 2013. Differential root proteome expression in tomato genotypes with contrasting drought tolerance exposed to dehydration. *Journal of the American Society for Horticultural Science* 138:131–41
31. Zhou S, Okekeogbu I, Sangireddy S, Ye Z, Li H, et al. 2016. Proteome modification in tomato plants upon long-term aluminum treatment. *Journal of Proteome Research* 15:1670–84
32. Joung JG, Corbett AM, Fellman SM, Tieman DM, Klee HJ, et al. 2009. Plant MetGenMAP: an integrative analysis system for plant systems biology. *Plant Physiology* 151:1758–68
33. Szklarczyk D, Gable AL, Lyon D, Junge A, Wyder S, et al. 2019. STRING v11: protein–protein association networks with increased coverage, supporting functional discovery in genome-wide experimental datasets. *Nucleic Acids Research* 47:D607–D613
34. Doncheva NT, Morris JH, Gorodkin J, Jensen LJ. 2019. Cytoscape StringApp: network analysis and visualization of proteomics data. *Journal of Proteome Research* 18:623–32
35. Flower DR, North ACT, Sansom CE. 2000. The lipocalin protein family: structural and sequence overview. *Biochimica et Biophysica Acta* 1482:9–24
36. Bharti K, Schmidt E, Lyck R, Heerklotz D, Bublak D, et al. 2000. Isolation and characterization of HsfA3, a new heat stress transcription factor of *Lycopersicon peruvianum*. *The Plant Journal* 22:355–65
37. Friedrich T, Oberkofler V, Trindade I, Altmann S, Brzezinka K, et al. 2021. Heteromeric HsFA2/HsFA3 complexes drive transcriptional memory after heat stress in *Arabidopsis*. *Nature Communications* 12:1–15
38. Scharf KD, Heider H, Höhfeld I, Lyck R, Schmidt E, et al. 1998. The tomato Hsf system: HsfA2 needs interaction with HsfA1 for efficient nuclear import and may be localized in cytoplasmic heat stress granules. *Molecular and Cellular Biology* 18:2240–51
39. Fragkostefanakis S, Mesihovic A, Simm S, Paupière MJ, Hu Y, et al. 2016. HsfA2 controls the activity of developmentally and stress-regulated heat stress protection mechanisms in tomato male reproductive tissues. *Plant Physiology* 170:2461–77
40. Liu HC, Charng YY. 2013. Common and distinct functions of *Arabidopsis* class A1 and A2 heat shock factors in diverse abiotic stress responses and development. *Plant physiology* 163:276–90
41. Charng YY, Liu HC, Liu NY, Chi WT, Wang CN, et al. 2007. A heat-inducible transcription factor, HsfA2, is required for extension of acquired thermotolerance in *Arabidopsis*. *Plant Physiology* 143:251–62
42. Schramm F, Ganguli A, Kiehlmann E, Englich G, Walch D, et al. 2006. The heat stress transcription factor HsfA2 serves as a regulatory amplifier of a subset of genes in the heat stress response in *Arabidopsis*. *Plant Molecular Biology* 60:759–72
43. Dahiya S, Saini V, Kumar P, Kumar A. 2019. Protein-Protein interaction network analyses of human WNT proteins involved in neural development. *Bioinformatics* 15:307
44. Keller M, SPOT-ITN Consortium, Simm S. 2018. The coupling of transcriptome and proteome adaptation during development and heat stress response of tomato pollen. *BMC Genomics* 19:1–20
45. Mittler R, Finka A, Goloubinoff P. 2012. How do plants feel the heat? *Trends in Biochemical Sciences* 37:118–25
46. Al-Wahaibi MH. 2011. Plant heat-shock proteins: a mini review. *Journal of King Saud University - Science* 23:139–50
47. Ding H, Mo S, Qian Y, Yuan G, Wu X, et al. 2020. Integrated proteome and transcriptome analyses revealed key factors involved in tomato (*Solanum lycopersicum*) under high temperature stress. *Food and Energy Security* 9:e239
48. Fragkostefanakis S, Simm S, Paul P, Bublak D, Scharf KD, et al. 2015. Chaperone network composition in *Solanum lycopersicum* explored by transcriptome profiling and microarray meta-analysis. *Plant, Cell & Environment* 38:693–709
49. Bitá CE, Zenoni S, Vriezen WH, Mariani C, Pezzotti M, et al. 2011. Temperature stress differentially modulates transcription in meiotic anthers of heat-tolerant and heat-sensitive tomato plants. *BMC Genomics* 12:384
50. Frank G, Pressman E, Ophir R, Althan L, Shaked R, et al. 2009. Transcriptional profiling of maturing tomato (*Solanum lycopersicum* L.) microspores reveals the involvement of heat shock proteins, ROS scavengers, hormones, and sugars in the heat stress response. *Journal of Experimental Botany* 60:3891–908
51. Männistö PT, Venäläinen J, Jalkanen A, García-Horsman JA. 2007. Prolyl oligopeptidase: a potential target for the treatment of cognitive disorders. *Drug News & Perspectives* 20:293–305
52. Jegadeesan S, Chaturvedi P, Ghatak A, Pressman E, Meir S, et al. 2018. Proteomics of heat-stress and ethylene-mediated thermotolerance mechanisms in tomato pollen grains. *Frontiers in Plant Science* 9:1558
53. Bang S, Min CK, Ha NY, Choi MS, Kim IS, et al. 2016. Inhibition of eukaryotic translation by tetratricopeptide-repeat proteins of *Orientia tsutsugamushi*. *Journal of Microbiology* 54:136–44
54. Ohashi-Ito K, Oda Y, Fukuda H. 2010. *Arabidopsis* VASCULAR-RELATED NAC-DOMAIN6 directly regulates the genes that govern programmed cell death and secondary wall formation during xylem differentiation. *The Plant Cell* 22:3461–73
55. Cao W, Liu N, Tang S, Bao L, Shen L, et al. 2008. Acetyl-Coenzyme A acyltransferase 2 attenuates the apoptotic effects of BNP3 in two human cell lines. *Biochimica et Biophysica Acta* 1780:873–80
56. Charng YY, Liu HC, Liu NY, Hsu FC, Ko SS. 2006. *Arabidopsis* Hsa32, a novel heat shock protein, is essential for acquired thermotolerance during long recovery after acclimation. *Plant Physiology* 140:1297–305
57. Hooper JD, Nicol DL, Dickinson JL, Eyre HJ, Scarman AL, et al. 1999. Testisin, a new human serine proteinase expressed by premeiotic testicular germ cells and lost in testicular germ cell tumors. *Cancer Research* 59:3199–205
58. Hinek A. 1996. Biological roles of the non-integrin elastin/laminin receptor. *Biological Chemistry* 377:471–80
59. Bokszczanin KL, Solanaceae Pollen Thermotolerance Initial Training Network (SPOT-ITN) Consortium, Fragkostefanakis S. 2013. Perspectives on deciphering mechanisms underlying plant heat stress response and thermotolerance. *Frontiers in Plant Science* 4:315
60. Liu H, Yu C, Li H, Ouyang B, Wang T, et al. 2015. Overexpression of *ShDHN*, a dehydrin gene from *Solanum habrochaites* enhances tolerance to multiple abiotic stresses in tomato. *Plant Science* 231:198–211
61. Hirose T, Hashida Y, Aoki N, Okamura M, Yonekura M, et al. 2014. Analysis of gene-disruption mutants of a sucrose phosphate synthase gene in rice, *OsSPS1*, shows the importance of sucrose synthesis in pollen germination. *Plant Science* 225:102–6
62. Santiago JP, Sharkey TD. 2019. Pollen development at high temperature and role of carbon and nitrogen metabolites. *Plant, Cell & Environment* 42:2759–75
63. Yu J, Loh K, Song ZY, Yang HQ, Zhang Y, et al. 2018. Update on glycerol-3-phosphate acyltransferases: the roles in the development of insulin resistance. *Nutrition & Diabetes* 8:1–10
64. Ischebeck T, Valledor L, Lyon D, Gingl S, Nagler M, et al. 2014. Comprehensive cell-specific protein analysis in early and late pollen development from diploid microsporocytes to pollen tube growth. *Molecular & Cellular Proteomics* 13:295–310
65. Tang X, Zhang Z, Zhang W, Zhao X, Li X, et al. 2010. Global gene profiling of laser-captured pollen mother cells indicates molecular pathways and gene subfamilies involved in rice meiosis. *Plant Physiology* 154:1855–1870
66. Panigrahi SK, Manterola M, Wolgemuth DJ. 2017. Meiotic failure in cyclin A1-deficient mouse spermatocytes triggers apoptosis through intrinsic and extrinsic signaling pathways and 14-3-3 proteins. *PLoS One* 12:e0173926

67. Kawai-Yamada M, Jin L, Yoshinaga K, Hirata A, Uchimiya H. 2001. Mammalian Bax-induced plant cell death can be down-regulated by overexpression of *Arabidopsis Bax Inhibitor-1 (AtBI-1)*. *PNAS* 98:12295–300
68. Ide M, Masuda K, Tsugama D, Fujino K. 2019. Death of female flower microsporocytes progresses independently of meiosis-like process and can be accelerated by specific transcripts in *Asparagus officinalis*. *Scientific Reports* 9:2703
69. Singh MB, Lohani N, Bhalla PL. 2021. The Role of endoplasmic reticulum stress response in pollen development and heat stress tolerance. *Frontiers in Plant Science* 12:661062
70. Yang Y, Ma F, Liu Z, Su Q, Liu Y, et al. 2019. The ER-localized Ca²⁺-binding protein calreticulin couples ER stress to autophagy by associating with microtubule-associated protein 1A/1B light chain 3. *Journal of Biological Chemistry* 294:772–82
71. Buchberger A, Bukau B, Sommer T. 2010. Protein quality control in the cytosol and the endoplasmic reticulum: brothers in arms. *Molecular Cell* 40:238–52
72. Hartl FU, Bracher A, Hayer-Hartl M. 2011. Molecular chaperones in protein folding and proteostasis. *Nature* 475:324–32
73. Li L, Lü S, Li R. 2017. The *Arabidopsis* endoplasmic reticulum associated degradation pathways are involved in the regulation of heat stress response. *Biochemical and Biophysical Research Communications* 487:362–67
74. Sugio A, Dreos R, Aparicio F, Maule AJ. 2009. The cytosolic protein response as a subcomponent of the wider heat shock response in *Arabidopsis*. *The Plant Cell* 21:642–54
75. Gidalevitz T, Prahlad V, Morimoto RI. 2011. The stress of protein misfolding: from single cells to multicellular organisms. *Cold Spring Harbor Perspectives in Biology* 3:a009704
76. Kobayashi T, Kobayashi E, Sato S, Hotta Y, Miyajima N, et al. 1994. Characterization of cDNAs induced in meiotic prophase in lily microsporocytes. *DNA Research* 1:15–26
77. Glover J, Grelon M, Craig S, Chaudhury A, Dennis E. 1998. Cloning and characterization of MS5 from *Arabidopsis*: a gene critical in male meiosis. *The Plant Journal* 15:345–56
78. Crickard JB, Kaniecki K, Kwon Y, Sung P, Greene EC. 2018. Meiosis-specific recombinase Dmc1 is a potent inhibitor of the Srs2 antirecombinase. *PNAS* 115:E10041–E10048



Copyright: © 2022 by the author(s). Published by Maximum Academic Press, Fayetteville, GA. This article is an open access article distributed under Creative Commons Attribution License (CC BY 4.0), visit <https://creativecommons.org/licenses/by/4.0/>.